Measurement of nonlinear optical coefficients by phase-matched harmonic generation

Robert C. Eckardt and Robert L. Byer
Ginzton Laboratory, Stanford University
Stanford CA 94305-4085

ABSTRACT

A wide range of nonlinear optical coefficients and various systems of notation have been used to describe optical second-harmonic generation (SHG). To avoid possible confusion, the techniques of optical nonlinear coefficient measurement and the elementary theory of SHG are briefly reviewed. Absolute and relative nonlinear coefficient measurements by phase-matched SHG are described. The following results were obtained: d_{36}(KDP) = 0.38 pm/V, d_{36}(KD*P) = 0.37 pm/V, $|d_{22}(BaB_2O_4)|$ = 2.2 pm/V, $d_{31}(LiIO_3)$ = −4.1 pm/V, $d_{31}(5\%MgO:LiNbO_3)$ = −4.7 pm/V, $|d_{15}$(KTP)| = 1.9 pm/V and $|d_{24}$(KTP)| = 3.5 pm/V. The accuracy of these measurements is estimated to be better than 10%. An example of high-repetition-rate pulsed SHG in $AgGaSe_2$ is given to demonstrate the use of quantitative analysis of harmonic generation for evaluation of nonlinear optical material performance.

1. INTRODUCTION

More accurate determination of second-order nonlinear optical coefficients is both possible and necessary with the higher optical quality that has become available in laser radiation and nonlinear optical materials. The output of early high power lasers was irregular in temporal and spatial distributions. The irregular nature of these lasers made absolute measurements of nonlinear optical coefficients difficult. Lasers with single-temporal-mode and single-spatial-mode output are becoming common in both high-power-pulsed and continuous wave (cw) operation. It is surprizing that uncertainty and disagreement about the values of nonlinear optical coefficients has persisted. Accurate absolute values are important. Quantitative analysis of nonlinear optical frequency conversion processes is a useful diagnostic tool for determining optimum conditions and avoiding effects that degrade the frequency conversion process. The uncertainty in the nonlinear optical coefficients, however, has made it difficult to perform accurate engineering calculations for nonlinear optical frequency conversion processes.

This paper reviews some recent measurements of nonlinear optical coefficients by the technique of phase-matched harmonic generation.[1] Phase-matched harmonic generation is one of several techniques of measurement and has an advantage of being performed under conditions that are closer to the conditions of practical applications than other techniques. Absolute measurements derived from phase-matched harmonic generation require careful characterization of the pump radiation and detailed attention to phase matching. It is necessary to provide a brief theoretical description to establish the definition of the nonlinear optical coefficient. This is done by reviewing harmonic conversion of monochromatic plane waves. Correlation with the focused Gaussian beam analysis of Boyd and Kleinman [2] and a simple extension to pulsed pumping provide the theory necessary for discussion of the experimental measurements.

TABLE I. SOME REPORTED VALUES FOR THE NONLINEAR OPTICAL COEFFICIENT d_{36} OF KDP

Singh in *CRC Handbook of Lasers*, 1971 [13]:
d_{36} = 0.473 pm/V at 1.06 μm
Singh in *CRC Handbook of Laser Science and Technology*, vol. III, 1986 [10]:
d_{36} = 0.41 pm/V at 1.06 μm
Levine & Betha, *Appl. Phys. Lett.* **20**, p. 272, 1972 [11]:
$d_{36} = 1.04\times10^{-9}$ (esu) at 1.318 μm
$d_{36}(\text{MKS}) = \frac{4\pi}{3\times10^4} d_{36}(\text{esu}) = 0.44$ pm/V
Kurtz, Jerphagnon & Choy, *Landolt-Börnstein*, 1979 [12]:
$\delta_{36} = 4.0\times10^{-2}$ m²/C
$d_{ijk} = \varepsilon_o \chi_{ii}^{(2\omega)} \chi_{jj}^{(\omega)} \chi_{kk}^{(\omega)} \delta_{ijk}$, $\chi = n^2 - 1$
d_{36} = 0.60 pm/V at 1.318 μm
= 0.63 pm/V at 1.06 μm
= 0.70 pm/V at 0.694 μm
Craxton, *IEEE J. Quant. Elect.* **QE-17**, p. 1771, 1981 [5]:
$(d_{36}/\varepsilon_o)_{\text{Craxton}}$ = 0.78 pm/V for SHG & THG
$d_{36} = (1/2)(d_{36}/\varepsilon_o)_{\text{Craxton}}$ = 0.39 pm/V
Yariv & Yeh, *Optical Waves in Crystals*, 1984 [14]:
$(d_{36})_{Y\&Y} = 0.50\times(1/9)\times10^{-22}$(MKS)
$d_{36} = (d_{36})_{Y\&Y}/\varepsilon_o$ = 0.63 pm/V
Eimerl, *Ferroelectrics* **72**, p. 95, 1987 [15]:
d_{36} = 0.39 pm/V
Shen, *The Principles of Nonlinear Optics*, 1984 [16]:
$\chi_{ii}^{(2)} = 0.94\times10^{-8}\times3/(4\pi)$ (esu), d_{36} = 0.47 pm/V
This work [1]:
d_{36} = 0.38 pm/V at 1.06 μm

The measurements reported here were initiated because of an inconsistency between the calculated threshold for oscillation in a BaB_2O_4 (BBO) optical parametric oscillator (OPO) and a lower observed threshold.[3] The value of the nonlinear coefficient of BBO [4] that was used for the OPO

threshold calculation was relative to KH_2PO_4 (KDP). Some controversy exists concerning the value of the nonlinear coefficient of KDP. A sampling of the reported values of the nonlinear optical coefficient of KDP is shown in Table I. Even for this widely used material there are a range of values. Using the same definition for nonlinear coefficient, the values fall into two groups. The group with lower values have absolute scales derived from phase-matched second-harmonic generation with either direct measurements of KDP [5, 1] or relative to absolute phase-matched harmonic generation measurements with $NH_4H_2PO_4$ (ADP). [6, 7] A second group with higher values of nonlinear coefficients are based on an absolute scale obtained by parametric florescence measurements on $LiIO_3$. [8, 9] Numerous other interrelations between previous measurements can be found in the tabulations of nonlinear optical coefficients. [10, 11, 12]

The nonlinear coefficient measurements presented here were expanded to include six materials: BBO, KDP, KD_2PO_4 (KD^*P), $LiIO_3$, 5%MgO:$LiNbO_3$, and $KTiOPO_4$ (KTP). Absolute measurements were made of the nonlinear optical coefficients of each of these materials. Relative measurements were also performed between the materials. This provided independence of earlier published results when comparing crystals. A overview of techniques for the measurement of nonlinear optical coefficients in presented in section 2. A brief discussion of the theory of second harmonic generation is presented in section 3 to establish the definition and notation that are used here. The measurements including characterization of pump radiation and phase matching are discussed in section 4. An example of quantitative analysis of second-harmonic generation in $AgGaSe_2$ is described in section 5.

2. MEASUREMENT TECHNIQUES

Measurement techniques for second-order nonlinear optical coefficients are reviewed briefly by Singh [10] and in more detail by Kurtz.[17] Here only a brief mention of the most often used techniques is made. The powder technique is useful for survey investigations, can indicate if harmonic generation is phase matchable, and yield a rough indication of the size of the nonlinear coefficient.[18] Small polished spheres or ellipsoids of nonlinear crystals are also good for survey measurements and determination of phase matching properties.[19] Harmonic generation in these tiny oriented polished crystals can yield an absolute measurement of effective nonlinear coefficient, but accuracy is limited. More accurate measurements require larger high-optical-quality crystals of the nonlinear optical material. The techniques used with the larger crystals include Maker fringe, wedge, phase-matched second-harmonic generation and parametric fluorescence.

In the Maker-fringe technique, harmonic generation is observed as the number of coherence lengths is changed by rotating the crystal. The harmonic signal will oscillate between a minimum and a maximum value as the crystal rotates and the number of coherence lengths change through integer values. The angular spacing of the Maker fringes can be used to determine the coherence length, and the peak harmonic intensity determines the nonlinear optical coefficient. The Maker-fringe technique can yield individual components of the nonlinear optical coefficient tensor when the proper polarizations are selected and the crystal is properly oriented. The wedge technique is similar to the Maker-fringe technique, but the number of coherence lengths is changed by translating the wedged sample and avoiding some problems associated with rotation. The wedge and Maker-fringe techniques are normally used for relative measurements referenced to a standard.

The technique of parametric fluorescence permits absolute measurements of nonlinear optical coefficients by the measurement of the ratio of pump power and parametric fluorescence power. It is not necessary to measure the absolute powers, but the ratio of powers must be measured precisely, and the power of the pump beam and the parametric fluorescence typically differ by eight orders of magnitude. It is necessary to accurately determine transmission and angular acceptance of the monochromator used to separate fluorescence from the pump radiation. Parametric amplification is a phase-matched process, and it is necessary to have constant phase-matching conditions throughout the crystal. Phase-matched measurements yield effective nonlinear optical coefficients, which are dependent on the direction of propagation through the crystal, possibly more the one component of the nonlinear optical coefficient tensor, and the polarization type of the parametric process.

Phase-matched second-harmonic generation can provide either absolute or relative measurement of the effective nonlinear coefficient. Precisely controlled phase matching is required. Accurate measurement of the of the incident and generated harmonic powers are required for absolute measurement of the nonlinear optical coefficient. Careful spatial, temporal, and spectral characterization of the fundamental radiation is also necessary for absolute measurements, and it is necessary to pay close attention to a number of other effects important at high intensity. Single-mode pulsed and cw lasers are becoming routinely available simplifying the characterization of the pump radiation and the analysis of the measurements.

Practical nonlinear optical frequency conversion applications provide a final check of the measured values. In many cases high efficiency harmonic generation, optical parametric oscillator thresholds, resonant cavity harmonic generation, and sum and difference frequency generation are too convoluted to serve as direct measurement techniques, but they provide a check of values. Indeed, OPO threshold observations provided the motivation to begin these measurements.

3. ELEMENTARY SECOND HARMONIC GENERATION THEORY

The theory of optical harmonic generation [20, 2] is well established and has been extensively reviewed.[21] There is, however, a wide range of notation in nonlinear optics, and different definitions of the nonlinear optical coefficient are used. Standardization of the definition is evolving, but for clarity some elementary theory is reviewed to make the definition explicit. This review is extended to show the relationship between the monochromatic planewave treatment of harmonic generation and the focused Gaussian beam analysis, and an approximation for pulsed harmonic conversion is presented.

The electric field and electric polarization, both of which are real, can be expressed as products of complex amplitudes and exponentials summed with the complex conjugates of those products. In this format the time dependent electric field of a monochromic planewave of angular frequency ω is

$$\boldsymbol{E}(\boldsymbol{r},t) = \frac{1}{2}\boldsymbol{E}(\boldsymbol{r},\omega)\exp\{i(\boldsymbol{k}\cdot\boldsymbol{r} - \omega t)\} + \text{c.c.} \tag{1}$$

The bold characters indicate vector quantities. The relationship expressing the vector components of the electric polarization at the harmonic frequency $\mathcal{P}_i^{NL}(\boldsymbol{r},2\omega)$ generated by the components of the fundamental electric field

$$\mathcal{P}_i^{NL}(\boldsymbol{r},2\omega) = \sum_{j,k=1}^{3}\varepsilon_0\, d_{ijk}(-2\omega,\omega,\omega)E_j(\boldsymbol{r},\omega)E_k(\boldsymbol{r},\omega), \tag{2}$$

where ε_0 is the permittivity of free space, define the second order nonlinear optical coefficients $d_{jkl}(-2\omega,\omega,\omega)$. The reduced notation $d_{ijk} \rightarrow d_{im}$ allows the representation of the nonlinear optical coefficients in the customary 3 x 6 matrix. Further reduction to a single effective nonlinear coefficient d_{eff} dependent on nonlinear optical properties, phase matching, and crystal orientation is standard for modeling phase-matched second-harmonic generation. The relationships between the effective nonlinear coefficients and the components of the reduced matrix of coefficients is given in a number of places.[10, 22, 23] It is necessary to include the birefringent walkoff angle ρ in the calculation of effective nonlinear coefficient;[2] omitting walkoff would make a difference as large as 10% in some crystals we measured. With this notation the coupled equations describing harmonic generation for a monochromatic planewave propagating in the z direction are

$$\frac{d}{dz}E(z,2\omega) = i\,\kappa e^{-i\Delta kz}E^2(z,\omega) \quad \text{and} \tag{3a}$$

$$\frac{d}{dz}E(z,\omega) = i\,\kappa e^{i\Delta kz}E(z,2\omega)E^*(z,\omega)\,, \tag{3b}$$

where the wave vector mismatch is given by $\Delta k = k_{2\omega} - 2k_{\omega}$, and $\kappa = \omega\, d_{eff}/(n\,c)$ with n the index of refraction, c the speed of light, and d_{eff} the effective nonlinear optical coefficient.

The intensity of monochromatic radiation can be expressed as a function of the electric field

$$I(z,\omega) = \{\varepsilon_0 c\, n(\omega)/2\}|E(z,\omega)|^2\,. \tag{4}$$

The elementary solutions to Eqs. (3) can be expressed in terms of the initial fundamental intensity $I_{\omega}(0)$ and the harmonic intensity $I_{2\omega}(l)$ generated in a crystal of length l. For the case of perfect phase matching, $\Delta k = 0$, and only small depletion of the fundamental wave, the solution is

$$I_{2\omega}(l) = I_{\omega}(0)\Gamma^2 l^2\,, \tag{5}$$

where $\Gamma^2 = 2\kappa^2 I_{\omega}(0)/(cn\varepsilon_0)$. Two other elementary solutions are for the case of imperfect phase matching and small depletion,

$$I_{2\omega}(l) = I_{\omega}(0)\{\Gamma l \sin(\Delta k\, l/2)/(\Delta k\, l/2)\}^2 , \tag{6}$$

and for the case arbitrary depletion of the fundamental and perfect phasematching,

$$I_{2\omega}(l) = I_{\omega}(0)\tanh^2(\Gamma l) . \tag{7}$$

It is possible to apply the monochromatic plane wave solutions to harmonic conversion of a cw beam of Gaussian transverse distribution provided birefringent walkoff and diffraction effects are insignificant. The intensity of an incident fundamental beam of Gaussian spatial profile is described by

$$I_{\omega}(r, z=0) = I_0 \exp(-2r^2/w_0^2) , \tag{8}$$

where $r = (x^2 + y^2)^{1/2}$ is the transverse radial coordinate and w_0 is the beam amplitude radius. The total power in the incident fundamental beam is

$$P_{\omega}(z=0) = \int_0^{\infty} 2\pi r\, dr\, I_{\omega}(r, z=0) = \pi w_0^2 I_0 / 2 . \tag{9}$$

The application of the monochromatic plane wave analysis requires the parameter Γ to be taken as a function of transverse position

$$\Gamma^2(r) = \Gamma_0^2 \exp(-2r^2/w_0^2) \tag{10}$$

where $\Gamma_0^2 = \{2\kappa^2/(nc\varepsilon_0)\} I_0$.

In the simplest approximation of small pump depletion and perfect phase matching, the harmonic power generated by a Gaussian fundamental beam in a crystal of length l is obtained by integrating Eq. (5) over the transversed spatial distribution of the beam

$$P_{2\omega}(l) = \frac{1}{2} P_{\omega}(0)\, \Gamma_0^2 l^2 = \frac{1}{2}\left(\frac{\omega d_{\text{eff}}}{nc}\right)^2 \left(\frac{2}{nc\varepsilon_0}\right) \frac{P_{\omega}^2(0)\, l^2}{\pi w_0^2/2} . \tag{11}$$

Allowances must be made for surfaces losses and bulk absorption losses not considered in Eq. (11). This equation is applicable for conditions of perfect phase matching, small pump depletion, and insignificant diffraction and birefringent walkoff.

Birefringent walkoff and diffraction are included in the Boyd and Kleinman analysis of harmonic generation [2] through the use of the focusing factor $h_m(B,\xi)$. The arguments of the function are the double refraction parameter $B = \rho (l k_{\omega})^{1/2}/2$ and the focusing parameter $\xi = l/b$ where ρ is the birefringent walkoff angle, l is the length of the nonlinear material, $k_{\omega} = \{2\pi n(\omega)\}/\lambda_0$ is the magnitude of the fundamental wave vector in the material, and $b = w_0^2 k_{\omega}$ is the confocal parameter. The harmonic power generated by a cw fundamental beam focused to a beam waist radius of w_0 in the center of the crystal is

$$P_{2\omega}(l) = 2\omega^2 d_{\text{eff}}^2 P_{\omega}^2(0) l k_{\omega} h_m(B,\xi)/\{\pi n^3 \varepsilon_0 c^3\} . \tag{12}$$

This is Eq. (2.22) of Ref. [2] specialized to the case of optimum phase matching with (2.29) of [2] and converted to MKS units. The focusing factor can be obtained from approximations valid in certain limiting conditions, from numerical integration, or from graphic representations of numerical evaluations. With substitution of the approximation $h_m(B,\xi) \approx \xi = l/w_0^2 k_{\omega}$, valid in the near field limit $\xi << 1$ and $B \to 0$, Eq. (12) reduces to Eq. (11). The approximation

$$h_m(B,\xi) \approx \xi (1 - t^2/12 + t^4/120 - t^6/1344 + \cdots) , \tag{13}$$

where $t = 2B(2\xi)^{1/2}$, is valid for weak focusing $\xi << 1$ with limited walkoff $\rho < l/\{w_0 \pi^{1/2}\}$, the condition used for most of the experimental measurements. Again absorption is not included in (13). A generalization of the focusing factor is required to deal with cases of non-optimum phase matching. This is necessary for the calculation of tuning curves for example. The generalization is given by Eqs. (2.22-24) and (2.16) of reference [2].

It is necessary to consider pulsed pump radiation and moderate levels of pump depletion in the analysis of the experimental data. The pulsed pump radiation was accommodated in the analysis by measuring the pulse shape with a fast detector and numerically integrating Eq. (12) over time using the observed pulse shape. Pump depletion was modeled with a near field approximation obtained from the monochromatic planewave analysis.

The monochromatic planewave analysis is useful for preliminary evaluation and also provides some useful insight. Application to pulsed harmonic generation requires that group velocity walkoff of the fundamental and harmonic is small compared to any temporal structure in addition to insignificant diffraction and birefringent walkoff. A simple model of the incident pulse is a Gaussian distribution in time and space

$$I_\omega(r,z=0,t) = I_0 \exp\{-2r^2/w_0^2 - 4t^2 \ln 2 / \Delta t^2\}, \tag{14}$$

where t is time and Δt is the full width in time at half maximum intensity. The total energy of this pulse is

$$U_\omega(z=0) = \int_0^\infty 2\pi r\, dr \int_{-\infty}^{\infty} dt\, I_\omega(r,z=0,t) = I_0 \frac{\pi w_0^2}{2} \sqrt{\frac{\pi}{\ln 2}} \frac{\Delta t}{2}. \tag{15}$$

Writing $\Gamma^2 = \Gamma_0^2 \exp\{-2r^2/w_0^2 - 4t^2 \ln 2/\Delta t^2\}$ where $\Gamma_0^2 = \{2\kappa^2/(n\, c\, \varepsilon_0)\} I_0^2$ and integrating the small-depletion perfectly phase-matched approximation of (5) over time and the transverse spatial distribution, the conversion efficiency of the incident fundamental energy $U_\omega(0)$ to harmonic energy $U_{2\omega}(l)$ generated in a crystal of length l is given by

$$\eta_0 = \frac{U_{2\omega}(l)}{U_\omega(0)} = \frac{1}{2\sqrt{2}} \Gamma_0^2 l^2 = \frac{2\sqrt{2 \ln 2}\, \omega^2 d_{\text{eff}}^2 U_\omega(0) l^2}{n^3 c^3 \varepsilon_0 \pi^{3/2} w_0^2 \Delta t}. \tag{16}$$

The symbol η_0 is used to represent conversion efficiency in the small depletion approximation. The same integration in time can be performed over the focussed Gaussian beam intensity conversion given by (12). The result is

$$\eta_0 = 2\omega^2 d_{\text{eff}}^2 \sqrt{2 \ln 2/\pi}\, U_\omega(0)\, l\, k_\omega\, h_m(B,\xi) / \{\pi n^3 \varepsilon_0 c^3 \Delta t\}. \tag{17}$$

An estimate conversion efficiency that takes depletion into consideration is given by

$$\eta_d \approx \eta_0/(1+\eta_0). \tag{18}$$

The approximation of (18) can be verified by numerical integration of the monochromatic planewave approximation with depletion and perfect phase matching given by (7); accuracy is better than 2%.

The definition of the nonlinear optical coefficients is stated in Eq. (2). Equations (3) or (5-7) also specify the notation and the definition. Different factors are used in various methods of presentation of optical harmonic generation, and care is required to avoid confusion. A correlation was made between the simpler monochromatic plane wave theory of SHG and the theory for focused Gaussian beams. The purpose was to provide a more intuitive understanding of the complicated mathematical expressions. Approximations to deal with pulsed fundamental radiation and depletion were presented. The expressions given here allow quantitative analysis of harmonic generation for a variety of conditions.

4. NONLINEAR OPTICAL COEFFICIENT MEASUREMENTS

Nonlinear coefficient measurements were performed in sets that involved the comparison of two crystals. One of the crystals was previously characterized and used as a reference, and the other crystal was the sample under test. The two beam experimental setup used for these measurements is shown schematically in Fig. 1. Harmonic generation with the two crystals was observed individually for absolute nonlinear optical coefficient measurements, and harmonic generation from the two crystals was compared for relative nonlinear coefficient measurements. Repeated calibration and characterization was used to assure accuracy.

The 1.064-μm pump radiation was generated by an single-mode injection-seeded Q-switched neodymium-doped yttrium aluminum garnet (Nd:YAG) laser. The laser output was characterized spatially, temporally, and spectrally. Two prisms were used to provide a spectral dispersion of 4 nm/mm to look for widely spaced spectral components. A knife-edge analysis of the beam transmitted through the prisms showed no additional spectral components. A Fabry-Perot etalon with 0.03 cm^{-1} spectral resolution was used to determine that the laser was oscillating in a single mode.

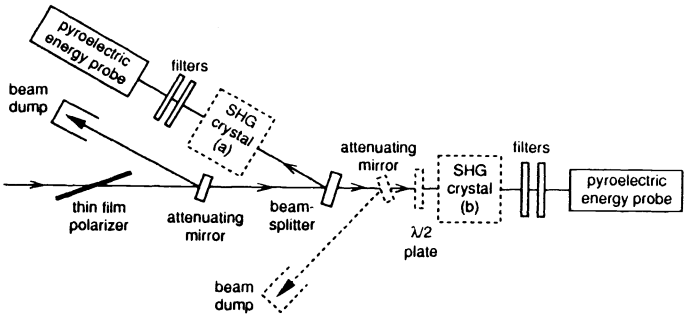

Fig. 1 Schematic of the experimental setup

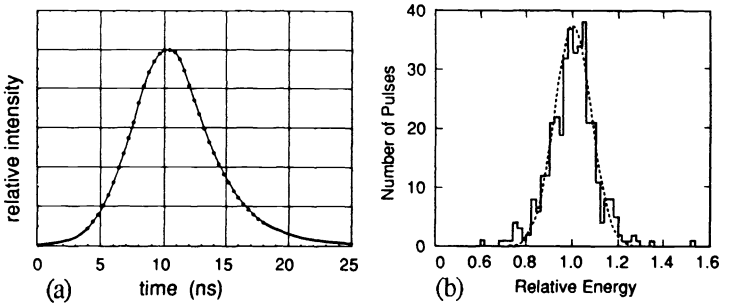

Fig. 2. (a) The fundamental pulse was sampled at 0.4-ns intervals, and the leading and trailing edges were represented as exponentials. (b) Histogram of single-shot pulse energy.

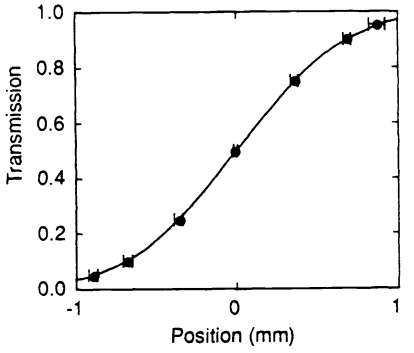

Fig. 3. Typical knife-edge measurement of transverse beam distribution at the crystal position. Data are averages of eight measurements with error bars. The solid line is the calculated transmission for as Gaussian distribution fit to the data.

When multimode oscillation occurred, it was also obvious in oscillograms. A photodiode-oscilloscope combination with 0.4-ns rise time was used to monitor pump pulse shape throughout the measurements. The time base of the oscilloscope was found to be accurate to better than 0.6% when tested with a mode-locked laser of precisely known repetition rate. The pump pulse had 7.0±2 ns full width at half maximum. The leading and trailing portions of the pump pulse were exponential with 1.4-ns rise time and 3.0-ns fall time. For analysis of harmonic generation, the central portion of the pulse was digitized from oscillograms, and the early rise and fall were treated as exponentials as shown in Fig. 2a. There was pulse-to-pulse energy fluctuation of the pump of ±8%; a histogram is shown in Fig. 2b. Harmonic generation data was recorded by averaging 100 pulses reducing the fluctuation of the averages by a factor of 10. The 8% shot-to-shot fluctuation will introduce a bias increasing average harmonic generation; this increase, however, is only 0.6%.

The laser output was transmitted though a spatial filter to produce a Gaussian-like beam. The beam was recollimated after the filter to place a beam waist adjusted in size between $w_0 = 0.9 - 1.6$ mm at the position of the crystals. It was verified that the propagation of the beam after transmission through the filter was that of a Gaussian beam. The vertical and horizontal beam distributions were measured several times during the course harmonic measurements by the knife edge technique. The edge positions for 5%, 10%, 25%, 50%, 75%, 90% and 95% transmission were observed. A beam waist size was obtained for the 6 positions other than 50%. Typically these six values agreed within ±3%, and over a day of measurements the values agreed within ±5%. An average of several knife-edge beam measurements is shown in Fig. 3. The uncertainty of beam size resulted in an error as large as the other sources of error combined for the nonlinear coefficient measurements.

Phase matching is of critical importance in second harmonic measurements of nonlinear coefficients. The crystals must be adjusted for optimum phase matching and phase matching must be uniform through the crystal. Each set of measurements required phase-matching tuning curves be observed for both reference and test crystals and compared with tuning curves calculated from dispersion equations. Observed and calculated tuning curves for $LiIO_3$ and $LiNbO_3$ are shown in Fig. 4. Lithium iodate is an angle-phase-matched crystal with 4.26° birefringent walkoff. The walkoff results in a change in the shape of the secondary maxima and minima of the tuning curve. The calculated tuning curves were obtained by numerical integration of Eqs. (2.16) and (2.24) of reference [2]. The curves shown in Figs. 4a and 4d show the combined fundamental and harmonic transmitted through the crystals as they were tuned through phase matching. The nearly constant transmission of the combined fundamental and harmonic shows that two-photon absorption of the harmonic radiation is not significant in these measurements.

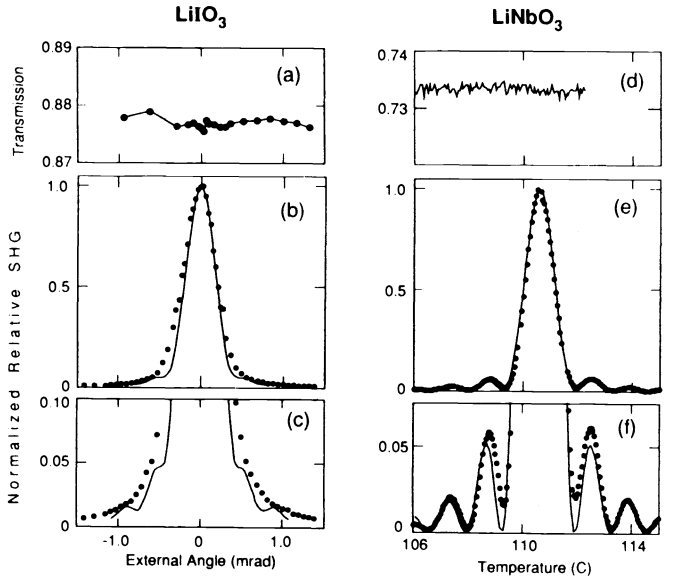

Fig. 4. The measures of phase-matching tuning for angle-tuned $LiIO_3$ and temperature tuned $LiNbO_3$ are shown as data points, and tuning curves calculated from dispersion equations are shown as the solid lines in (b,c) and (e,f). The measured total transmission of fundamental and harmonic as the two crystals are tuned through phase matching are shown in (a) and (d).

TABLE II.
NONLINEAR OPTICAL COEFFICIENTS

Crystal	Nonlinear optical coefficient[(a)] (10^{-12} m/V)
KDP	$d_{36} = 0.38$
KD*P	$d_{36} = 0.37$
$LiIO_3$	$d_{31} = -4.1$
5%MgO:$LiNbO_3$	$d_{31} = -4.7$
BaB_2O_4	$d_{eff} = 1.94$ $\|d_{22}\| = 2.2$[(b)]
KTP	$d_{eff} = 3.2$ $\|d_{15}\| = 1.9$[(c)] $\|d_{24}\| = 3.5$

(a) Nonlinear coefficients are given for 1064 to 532 nm second harmonic generation.

(b) Assumes that $|d_{31}| \ll |d_{22}|$ for BaB_2O_4 [27].

(c) Using $|d_{24}| / |d_{15}| = 1.8$ [25] and assuming d_{24} and d_{15} have the same sign.

A number of other checks and calibrations were performed. The intensity dependence of harmonic generation was observed by attenuating the fundamental beam. Only the pump depletion described by Eq. (18) was observed. There was no indication of two photon absorption or loss of phase matching due to intensity dependent index of refraction. The crystals were placed on mounts with 3 axes of rotation. Crystal orientation could be confirmed with polarized alignment beams, and crystal rotation confirmed that d_{eff} was maximum. The transmission of mirrors, beam splitters, and crystals was measured with a spectrophotometer and with the two beam experimental setup. A separate harmonic crystal was used for measuring transmissions and reflections at 532 nm in the two-beam setup. A half-wave plate was used to rotate polarization for maximum conversion in type-II crystals. Reproducibility of the nonlinear coefficient measurements was 4%, and this is relative accuracy of the measurements. The absolute values may have some bias. It is estimated that the absolute accuracy is 10%.

The results of the measurements are given in Table II. The agreement and disagreement with earlier published results illustrates the confusions that exists in the absolute values of nonlinear optical coefficients. The measurement for KDP is in agreement with the nonlinear coefficient accepted for that material in high-power nonlinear conversion applications,[15] and it agrees with the combination of relative measurements between KDP and $NH_4H_4PO_2$ (ADP) and low-power cw absolute second-harmonic measurements with ADP.[10] The ratios of values for KD*P and KDP and for $LiIO_3$ and KDP are in agreement with earlier measurements. The value of d_{31} for $LiIO_3$ reported here, however, is only 58% of the value obtained earlier by the technique of parametric fluorescence. The ratio of $d_{22}(BaB_2O_4)/d_{36}(KDP) = 5.8$ is larger than the value of 4.1 reported earlier. The value of d_{31}(5%MgO:$LiNbO_3$) = 4.7 pm/V is lower than the value 5.8 pm/V obtained by parametric fluorescence for congruent $LiNbO_3$,[9] but there is a compositional variation in the material involved. The value of d_{eff}(KTP) is more than a factor of two smaller than reported earlier

Substantiation of these results will come only when a consensus develops from nonlinear optical applications and further measurement. This consensus appears to be developing. We have received a number of private communications in agreement with these results. Recent publications describing optical parametric oscillator threshold in KTP [24, 25] and $LiIO_3$ [26] have shown agreement. Still much remains to be done. The variance between parametric fluorescence and second harmonic generation measurements needs to be resolved. With the current improvements in laser performance and the quality of nonlinear optical

materials it is appropriate that nonlinear optical frequency conversion be analyzed quantitatively. Such engineering design and analysis will be useful for characterizing materials, optimizing performance, and increasing the base of knowledge of properties of nonlinear optical materials.

5. SHG IN $AgGaSe_2$ AS AN EXAMPLE

The quantitative analysis of harmonic generation in silver selenogallate ($AgGaSe_2$) pumped by high repetition rate pulse CO_2 laser radiation was a predecessor to the measurements described above. The $AgGaSe_2$ measurements were performed in collaboration with Leon Newman and John Kennedy at United Technologies Research Center.[28] The useful spectral range of $AgGaSe_2$ for nonlinear frequency conversion is 1.5 - 12 μm determined by phase matching and transmission properties. The material angle phase matches at $\theta = 55°$ for 10.6- to 5.3-μm SHG. There is an interest in extending the use of this material to increased power levels. The SHG measurements demonstrated that when pumped by 20-ns 10.6-μm pulses of 100 kHz repetition rate $AgGaSe_2$ performed well for average intensity up to 200 kW/cm^2 for the bulk material and 20 kW/cm^2 for the surfaces. Surface damage occurred at intensities above 20 kW/cm^2. The measurements indicated that the lower value of the reported range of nonlinear coefficients 32.4 - 67.7 pm/V [10] is more accurate.

The continuously pumped, repetitively Q-switched CO_2 laser oscillated on a single cavity mode. The output was Gaussian-like both in spatial an temporal distribution. The output was monitored with 2-ns-rise-time HgCdTe detectors, beam distributions were measured with a translated knife-edge, and multiple energy probes were used to check calibration. Phase matching measurements displayed tuning curves very similar to those calculated for the 1.8-cm long crystal. This early material had 6% per cm loss coefficient mainly due to scattering. Material with at least an order of magnitude lower loss is available now. The pulse repetition rate of the laser could be varied up to 100 kHz where the average output power was 8.2 W. The fundamental beam was focused to beam waist radii from $w_0 = 47$ μm to 320 μm inside the crystal. The second-harmonic measurements were analyzed using the nonlinear coefficient $d_{36}(AgGaSe_2) = 32.4$ pm/V reported by Kildal and Mikkelsen [29] to obtain a value for the Boyd and Kleinman focusing factor $h_m(B,\xi)$. These values are compared with calculations using the double refraction parameter $B = 0.97$ for the 1.8-cm-long $AgGaSe_2$ crystal in Fig. 5. The agreement is good over a wide range of focusing conditions indicating that optical distortion is not significant at peak intensity as high as 90 MW/cm^2 at the focus in the bulk material. Harmonic-conversion efficiency is shown as a function of peak power in Fig. 6. The conversion efficiency even at the highest intensity of 74 MW/cm^2 decreases only as is expected from the depletion approximation given by Eq. (18).

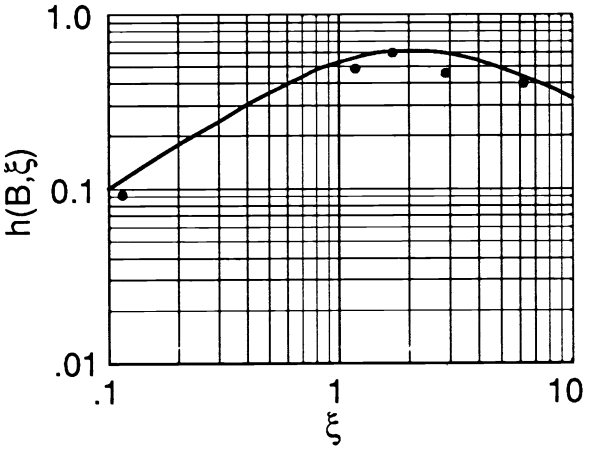

Fig. 5 The data points represent 10.6- to 5.3-μm second-harmonic generation in $AgGaSe_2$ for different focusing conditions represented as observed values of the Boyd and Kleinman focusing factor $h_m(B,\xi)$. The observed focusing factors were calculated using $d_{36}(AgGaSe_2) = 32.4$ pm/V and measured experimental conditions. The solid curve is the calculated focusing factor for the double refraction parameter $B = 0.97$ corresponding to a 1.8-cm-long $AgGaSe_2$ crystal. The abscissa is the focusing parameter $\xi = l/b = l\,(k_1 w_0^2)$.

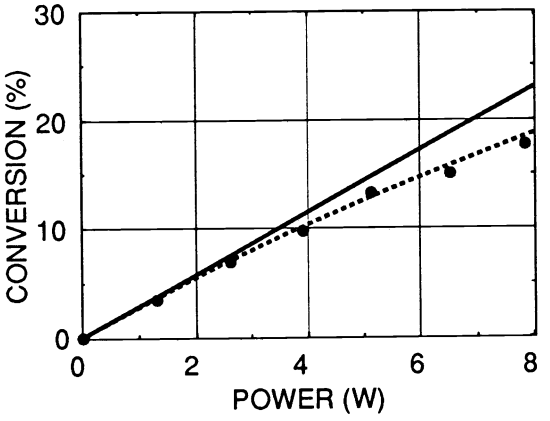

Fig. 6. The effects of pump depletion are seen as the fundamental power is increased for SHG in $AgGaSe_2$. The measurements were made with 20-ns 10.6-μm fundamental pulses with a repetition rate of 10 kHz. The fundamental was attenuated with a polarizer-analyzer pair to achieve different intensities. The solid line is the calculated conversion efficiency without pump depletion from Eq. (17). The dashed line includes the effect of depletion as estimated by equation (18).

A quantitative analysis of nonlinear frequency conversion such as this yields valuable information. There is an indication of the correct value of nonlinear coefficient when a range of values are reported. Damage thresholds for high-repetition-rate 20-ns pulses of fundamental radiation are determined. An it is shown that within these limits, harmonic conversion is not reduced by distortion or third order nonlinear effects in the crystal. With this information it is possible to proceed with engineering calculations to optimize frequency conversion. Such calculations are now possible and necessary with the good quality that is available in nonlinear optical materials and the laser outputs used to pump the nonlinear optical frequency conversion processes.

6. ACKNOWLEDGEMENTS

This work was supported by the U. S. Army Research Office contracts DAAL03-88-K-0113 and DAAL03-90-C-0026. It is a pleasure to acknowledge Hisashi Masuda and Yuan Xuan Fan for their participation in the nonlinear optical coefficient measurements, and Leon Newman and John Kennedy for collaboration on the $AgGaSe_2$ measurements. We also express our appreciation to the organizations and individuals who provided materials for this investigation. The barium metaborate crystals were supplied by R. Route and R. Feigelson of Stanford University and C.-T. Chen of the Fujian Institute. R. Route and R. Feigelson also grew the $AgGaSe_2$ crystals. S. Velsko of Lawrence Livermore National Laboratory loaned the KDP crystal. And the 5%MgO:$LiNbO_3$ material was supplied by Crystal Technology, Inc. of Palo Alto CA.

7. REFERENCES

1. R. C. Eckardt, H. Masuda, Y. X. Fan and R. L. Byer, IEEE J. Quantum Electron. **26**, pp. 922-933 (1990).
2. G. D. Boyd and D. A. Kleinman, J. Appl. Phys. **39**, pp. 3597-3639 (1968).
3. Y. X. Fan, R. C. Eckardt, R. L. Byer, C.-T. Chen and A. D. Jiang, IEEE J. Quantum Electron. **25**, pp. 1196-1199 (1989).
4. C.-T. Chen, Scintia Sinica **28**, pp. 235-243 (1985).
5. R. S. Craxton, IEEE J. Quantum Electron. **QE-17**, pp. 1771-1782 (1981).
6. G. E. Francois, Phys. Rev. **143**, pp. 597-600 (1966).
7. J. E. Bjorkholm and A. E. Siegman, Phys. Rev. **154**, pp. 851-860 (1967).
8. A. J. Campillo and C. L. Tang, Appl. Phys. Lett. **16**, pp. 242-244 (1970).
9. M. M. Choy and R. L. Byer, Phys. Rev. B **14**, pp. 1693-1706 (1976).
10. S. Singh, *Handbook of Laser Science*, edited by M. J. Weber (CRC, Boca Raton, Florida, 1986), pp. 3-228.
11. B. F. Levine and C. G. Bethea, Appl. Phys. Lett. **20**, pp. 272-275 (1972).
12. S. K. Kurtz, J. Jerphagagnon and M. M. Choy, *Landolt-Börnstein, Numerical Data and Functional Relationships in Science and Technology, Group III, Vol. 11*, edited by K.-H. Hellwege and A. M. Hellwege (Springer, Berlin, 1979), pp. 671-743.
13. S. Singh, *Handbook of Lasers with Selected Data on Optical Technology*, edited by R. J. Pressley (CRC, Cleveland, 1971), pp. 489-523.
14. A. Yariv and P. Yeh, *Optical Waves in Crystals* (Wiley, New York,1984).
15. D. Eimerl, Ferroelectrics **72**, pp. 95-139 (1987).
16. Y. R. Shen, *The Principles of Nonlinear Optics* (Wiley, New York,1984).
17. S. K. Kurtz, *Quantum Electronics, vol. I, part A*, edited by H. Rabin and C. L. Tang (Academic, New York, 1975), pp. 209-281.
18. S. K. Kurtz and T. T. Perry, J. Appl. Phys. **39**, pp. 3798-3813 (1968).
19. S. P. Velsko, Opt. Eng. **28**, pp. 76-84 (1989).
20. J. A. Armstrong, N. Bloembergen, J. Ducuing and P. S. Pershan, Phys. Rev. **127**, pp. 1918-1939 (1962).
21. S. A. Akhmanov, A. I. Kovrygin and A. P. Sukhorukov, *Quantum Electronics: a Treatise, vol. 1, part B*, edited by H. Rabin and C. L. Tang (Academic, New York, 1975), pp. 475-586.
22. R. L. Byer, *Nonlinear Optics*, edited by P. G. Harper and B. S. Wherrett (Academic, San Francisco, 1977), pp. 47-160.
23. F. Zernike and J. E. Midwinter, *Applied Nonlinear Optics* (Wiley, New York,1973).
24. L. R. Marshall, J. Kasinski, A. D. Hays and R. Burnham, Opt. Lett. **16**, pp. 681-683 (1991).
25. K. Kato, IEEE J. Quantum Electron. **27**, pp. 1137-1140 (1991).
26. P. F. Curley and A. I. Ferguson,Opt. Commun. **80**, pp. 365-369 (1991).
27. D. Eimerl, L. Davis, S. Velsko, E. K. Graham and A. Zalkin, J. Appl. Phys. Lett. **62**, pp. 1968-1983 (1987).
28. R. C. Eckardt, R. L. Byer, L. A. Newman and J. Kennedy, in Conference on Lasers and Electro-Optics Technical Digest Series 1988, Vol. 7(Optical Society of America, Washington, 1988), paper WM33.
29. H. Kildal and J. C. Mikkelsen, Opt. Commun. **9**, pp. 315-318 (1973).